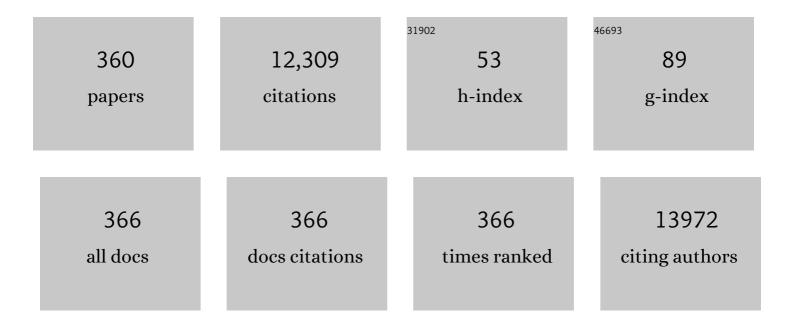
## Andrew Keith Whittaker

List of Publications by Year in descending order

Source: https://exaly.com/author-pdf/3328735/publications.pdf Version: 2024-02-01



#	Article	IF	CITATIONS
1	Comprehensive Study of Surface Chemistry of MCM-41 Using29Si CP/MAS NMR, FTIR, Pyridine-TPD, and TGA. Journal of Physical Chemistry B, 1997, 101, 6525-6531.	1.2	679
2	Minimum information reporting in bio–nano experimental literature. Nature Nanotechnology, 2018, 13, 777-785.	15.6	455
3	A Method for Estimating the Nature and Relative Proportions of Amorphous, Single, and Double-Helical Components in Starch Granules by13C CP/MAS NMR. Biomacromolecules, 2007, 8, 885-891.	2.6	337
4	High energy radiation grafting of fluoropolymers. Progress in Polymer Science, 2003, 28, 1355-1376.	11.8	330
5	Bioerodable PLGA-Based Microparticles for Producing Sustained-Release Drug Formulations and Strategies for Improving Drug Loading. Frontiers in Pharmacology, 2016, 7, 185.	1.6	255
6	Tailoring the Void Size of Iron Oxide@Carbon Yolk–Shell Structure for Optimized Lithium Storage. Advanced Functional Materials, 2014, 24, 4337-4342.	7.8	212
7	Solution Properties of Star and Linear Poly(N-isopropylacrylamide). Macromolecules, 2006, 39, 8379-8388.	2.2	179
8	Biological Utility of Fluorinated Compounds: from Materials Design to Molecular Imaging, Therapeutics and Environmental Remediation. Chemical Reviews, 2022, 122, 167-208.	23.0	172
9	Functional Hyperbranched Polymers: Toward Targeted <i>in Vivo</i> <sup>19</sup> F Magnetic Resonance Imaging Using Designed Macromolecules. Journal of the American Chemical Society, 2010, 132, 5336-5337.	6.6	168
10	Structure and Orientation of the Pore-forming Peptide Melittin, in Lipid Bilayers. Journal of Molecular Biology, 1994, 241, 456-466.	2.0	165
11	Multimodal Polymer Nanoparticles with Combined <sup>19</sup> F Magnetic Resonance and Optical Detection for Tunable, Targeted, Multimodal Imaging <i>in Vivo</i> . Journal of the American Chemical Society, 2014, 136, 2413-2419.	6.6	160
12	Rehydration process of milk protein concentrate powder monitored by static light scattering. Food Hydrocolloids, 2009, 23, 1958-1965.	5.6	150
13	Investigation of the microstructure of milk protein concentrate powders during rehydration: Alterations during storage. Journal of Dairy Science, 2010, 93, 463-472.	1.4	137
14	Nanoparticle-mediated local depletion of tumour-associated platelets disrupts vascular barriers and augments drug accumulation in tumours. Nature Biomedical Engineering, 2017, 1, 667-679.	11.6	132
15	The chemistry of novolac resins: 3. 13C and 15N n.m.r. studies of curing with hexamethylenetetramine. Polymer, 1997, 38, 5835-5848.	1.8	116
16	Structure of calcium aluminate sulfate Ca4Al6O16S. Journal of Solid State Chemistry, 1995, 119, 1-7.	1.4	107
17	Synthesis of Gadolinium-Labeled Shell-Crosslinked Nanoparticles for Magnetic Resonance Imaging Applications. Advanced Functional Materials, 2005, 15, 1248-1254.	7.8	99
18	Ultrasound evaluation of polymer gel dosimeters. Physics in Medicine and Biology, 2002, 47, 1449-1458.	1.6	98

2

#	Article	IF	CITATIONS
19	High F-Content Perfluoropolyether-Based Nanoparticles for Targeted Detection of Breast Cancer by <sup>19</sup> F Magnetic Resonance and Optical Imaging. ACS Nano, 2018, 12, 9162-9176.	7.3	98
20	Hydrophilic and Amphiphilic Polyethylene Glycol-Based Hydrogels with Tunable Degradability Prepared by "Click―Chemistry. Biomacromolecules, 2012, 13, 4012-4021.	2.6	96
21	Ultra-stable all-solid-state sodium metal batteries enabled by perfluoropolyether-based electrolytes. Nature Materials, 2022, 21, 1057-1065.	13.3	92
22	The relationship between radiation-induced chemical processes and transverse relaxation times in polymer gel dosimeters. Physics in Medicine and Biology, 2001, 46, 1061-1074.	1.6	90
23	Synthesis and Evaluation of Partly Fluorinated Block Copolymers as MRI Imaging Agents. Biomacromolecules, 2009, 10, 374-381.	2.6	88
24	Polymerization-Induced Self-Assembly (PISA) - Control over the Morphology of <sup>19</sup> F-Containing Polymeric Nano-objects for Cell Uptake and Tracking. Biomacromolecules, 2017, 18, 1145-1156.	2.6	86
25	Bioinspired Core–Shell Nanoparticles for Hydrophobic Drug Delivery. Angewandte Chemie - International Edition, 2019, 58, 14357-14364.	7.2	85
26	13C-NMR,1H-NMR, and FT-Raman study of radiation-induced modifications in radiation dosimetry polymer gels. Journal of Applied Polymer Science, 2001, 79, 1572-1581.	1.3	82
27	Investigation of ultrasonic properties of PAG and MAGIC polymer gel dosimeters. Physics in Medicine and Biology, 2002, 47, 4397-4409.	1.6	80
28	Molecular imaging of activated platelets via antibody-targeted ultra-small iron oxide nanoparticles displaying unique dual MRI contrast. Biomaterials, 2017, 134, 31-42.	5.7	78
29	The effects of particle size, shape, density and flow characteristics on particle margination to vascular walls in cardiovascular diseases. Expert Opinion on Drug Delivery, 2018, 15, 33-45.	2.4	77
30	An electron spin resonance study on Î <sup>3</sup> -irradiated poly(l-lactic acid) and poly(d,l-lactic acid). Polymer Degradation and Stability, 1995, 50, 297-304.	2.7	73
31	Electrospinning and crosslinking of low-molecular-weight poly(trimethylene carbonate-co-l-lactide) as an elastomeric scaffold for vascular engineering. Acta Biomaterialia, 2013, 9, 6885-6897.	4.1	71
32	Molecular weight changes and scission and crosslinking in poly(dimethyl siloxane) on gamma radiolysis. Radiation Physics and Chemistry, 2001, 62, 11-17.	1.4	70
33	Effect of Impurities in Cumyl Dithiobenzoate on RAFT-Mediated Polymerizations. Macromolecules, 2005, 38, 5352-5355.	2.2	69
34	Characteristics of starch-based films plasticised by glycerol and by the ionic liquid 1-ethyl-3-methylimidazolium acetate: A comparative study. Carbohydrate Polymers, 2014, 111, 841-848.	5.1	69
35	An Injectable Hydrogel for Simultaneous Photothermal Therapy and Photodynamic Therapy with Ultrahigh Efficiency Based on Carbon Dots and Modified Cellulose Nanocrystals. Advanced Functional Materials, 2021, 31, 2106079.	7.8	69
36	Localised delivery of doxorubicin to prostate cancer cells through a PSMA-targeted hyperbranched polymer theranostic. Biomaterials, 2017, 141, 330-339.	5.7	68

Т

#	ARTICLE	IF	CITATIONS
37	Determination of T1ÏH Relaxation Rates in Charred and Uncharred Wood and Consequences for NMR Quantitation. Solid State Nuclear Magnetic Resonance, 2002, 22, 50-70.	1.5	67
38	Rehydration of high-protein-containing dairy powder: Slow- and fast-dissolving components and storage effects. Dairy Science and Technology, 2010, 90, 335-344.	2.2	67
39	Novel iron oxide–cerium oxide core–shell nanoparticles as a potential theranostic material for ROS related inflammatory diseases. Journal of Materials Chemistry B, 2018, 6, 4937-4951.	2.9	67
40	pH-responsive star polymer nanoparticles: potential 19F MRI contrast agents for tumour-selective imaging. Polymer Chemistry, 2013, 4, 4480.	1.9	66
41	Biodegradable core crosslinked star polymer nanoparticles as <sup>19</sup> F MRI contrast agents for selective imaging. Polymer Chemistry, 2014, 5, 1760-1771.	1.9	66
42	The evolution of gadolinium based contrast agents: from single-modality to multi-modality. Nanoscale, 2016, 8, 10491-10510.	2.8	66
43	Analysis of lipoproteins using 2D diffusion-edited NMR spectroscopy and multi-way chemometrics. Analytica Chimica Acta, 2005, 531, 209-216.	2.6	64
44	Ultrasonic absorption in polymer gel dosimeters. Ultrasonics, 2003, 41, 551-559.	2.1	61
45	Cross-Linked Poly(trimethylene carbonate- <i>co</i> - <scp>l</scp> -lactide) as a Biodegradable, Elastomeric Scaffold for Vascular Engineering Applications. Biomacromolecules, 2011, 12, 3856-3869.	2.6	61
46	PFPE-Based Polymeric <sup>19</sup> F MRI Agents: A New Class of Contrast Agents with Outstanding Sensitivity. Macromolecules, 2017, 50, 5953-5963.	2.2	61
47	NMR study of the gamma radiolysis of poly(dimethyl siloxane) under vacuum at 303 K. Polymer, 2002, 43, 1051-1059.	1.8	60
48	The behavior of aged regenerated Bombyx mori silk fibroin solutions studied by 1H NMR and rheology. Biomaterials, 2008, 29, 4268-4274.	5.7	59
49	Protein Conformational Modifications and Kinetics of Waterâ^'Protein Interactions in Milk Protein Concentrate Powder upon Aging: Effect on Solubility. Journal of Agricultural and Food Chemistry, 2010, 58, 7748-7755.	2.4	58
50	Polymeric <sup>19</sup> F MRI agents responsive to reactive oxygen species. Polymer Chemistry, 2017, 8, 4585-4595.	1.9	57
51	Copolymer hydrogels of 2-hydroxyethyl methacrylate with n-butyl methacrylate and cyclohexyl methacrylate: synthesis, characterization and uptake of water. Polymer, 2000, 41, 1287-1296.	1.8	55
52	Miscibility and Specific Interactions in Blends of Poly(4-vinylphenol) and Poly(2-ethoxyethyl) Tj ETQqO 0 0 rgBT /(	Overlock 1	0 Tf 50 142 T
53	Investigation into the Diffusion of Water into HEMA-co-MOEP Hydrogels. Biomacromolecules, 2004, 5, 1194-1199.	2.6	54

Control of the Orientation of Symmetric Poly(styrene)-<i>block</i>-poly(<scp>d</scp>,<scp>l</scp>-lactide) Block Copolymers Using Statistical Copolymers of Dissimilar Composition. Langmuir, 2012, 28, 15876-15888. 54 1.6 53

#	Article	IF	CITATIONS
55	Development of a polymer theranostic for prostate cancer. Polymer Chemistry, 2014, 5, 6932-6942.	1.9	53
56	lon-Responsive <sup>19</sup> F MRI Contrast Agents for the Detection of Cancer Cells. ACS Sensors, 2016, 1, 757-765.	4.0	53
57	Ultrasensitive Magnetic Tuning of Optical Properties of Films of Cholesteric Cellulose Nanocrystals. ACS Nano, 2020, 14, 9440-9448.	7.3	53
58	The synthesis of waterâ€soluble PHEMA via ARGET ATRP in protic media. Journal of Polymer Science Part A, 2010, 48, 4084-4092.	2.5	52
59	Biocidal Polymers: A Mechanistic Overview. Polymer Reviews, 2017, 57, 276-310.	5.3	52
60	Surface-Functionalized Polymer Nanoparticles for Selective Sequestering of Heavy Metals. Advanced Materials, 2006, 18, 582-586.	11.1	51
61	A hybrid sodium-ion capacitor with polyimide as anode and polyimide-derived carbon as cathode. Journal of Power Sources, 2018, 396, 12-18.	4.0	51
62	Segmented Highly Branched Copolymers: Rationally Designed Macromolecules for Improved and Tunable <sup>19</sup> F MRI. Biomacromolecules, 2015, 16, 2827-2839.	2.6	50
63	Enhanced Performance of Polymeric <sup>19</sup> F MRI Contrast Agents through Incorporation of Highly Water-Soluble Monomer MSEA. Macromolecules, 2018, 51, 5875-5882.	2.2	50
64	Integrating Fluorinated Polymer and Manganese‣ayered Double Hydroxide Nanoparticles as pHâ€activated <sup>19</sup> F MRI Agents for Specific and Sensitive Detection of Breast Cancer. Small, 2019, 15, e1902309.	5.2	49
65	Strong, Ultrafast, Reprogrammable Hydrogel Actuators with Muscle-Mimetic Aligned Fibrous Structures. Chemistry of Materials, 2021, 33, 7818-7828.	3.2	49
66	Activatable magnetic resonance nanosensor as a potential imaging agent for detecting and discriminating thrombosis. Nanoscale, 2018, 10, 15103-15115.	2.8	46
67	Synthesis and evaluation of partly fluorinated polyelectrolytes as components in 19F MRI-detectable nanoparticles. Polymer Chemistry, 2010, 1, 1039.	1.9	45
68	Synthesis and Characterization of a POSS-PEG Macromonomer and POSS-PEG-PLA Hydrogels for Periodontal Applications. Biomacromolecules, 2014, 15, 666-679.	2.6	45
69	Controllable synthesis of up-conversion nanoparticles UCNPs@MIL-PEG for pH-responsive drug delivery and potential up-conversion luminescence/magnetic resonance dual-mode imaging. Journal of Alloys and Compounds, 2018, 749, 939-947.	2.8	45
70	Polymer Electrode Materials for Sodium-ion Batteries. Materials, 2018, 11, 2567.	1.3	45
71	Tailored Polyimide–Graphene Nanocomposite as Negative Electrode and Reduced Graphene Oxide as Positive Electrode for Flexible Hybrid Sodium-Ion Capacitors. ACS Applied Materials & Interfaces, 2018, 10, 43730-43739.	4.0	45
72	Carbon structure and porosity of carbonaceous adsorbents in relation to their adsorption properties. Carbon, 1999, 37, 1491-1497.	5.4	44

Andrew Keith Whittaker

#	Article	IF	CITATIONS
73	Protein delivery using nanoparticles based on microemulsions with different structure-types. European Journal of Pharmaceutical Sciences, 2008, 33, 434-444.	1.9	44
74	Molecular Motion in Miscible Polymer Blends. 1. Motion in Blends of PEO and PVPh Studied by Solid-State13CT1ïMeasurements. Macromolecules, 1997, 30, 3560-3568.	2.2	43
75	1H NMR Study of the States of Water in Equilibrium Poly(HEMA-co-THFMA) Hydrogels. Biomacromolecules, 2002, 3, 991-997.	2.6	43
76	Pyromellitic dianhydride-based polyimide anodes for sodium-ion batteries. Electrochimica Acta, 2018, 265, 702-708.	2.6	43
77	Sulfoxideâ€Containing Polymerâ€Coated Nanoparticles Demonstrate Minimal Protein Fouling and Improved Blood Circulation. Advanced Science, 2020, 7, 2000406.	5.6	43
78	Antifouling Surfaces Enabled by Surface Grafting of Highly Hydrophilic Sulfoxide Polymer Brushes. Biomacromolecules, 2021, 22, 330-339.	2.6	43
79	Hyperbranched polymers as delivery vectors for oligonucleotides. Journal of Polymer Science Part A, 2012, 50, 2585-2595.	2.5	42
80	A unique <sup>19</sup> F MRI agent for the tracking of non phagocytic cells <i>in vivo</i> . Nanoscale, 2018, 10, 8226-8239.	2.8	42
81	Water characteristics in cooked beef as influenced by ageing and high-pressure treatment—an NMR micro imaging study. Meat Science, 2004, 66, 301-306.	2.7	41
82	In Situ Techniques for Developing Robust Li–S Batteries. Small Methods, 2018, 2, 1800133.	4.6	41
83	Carbon dots embedded metal organic framework @ chitosan core-shell nanoparticles for vitro dual mode imaging and pH-responsive drug delivery. Microporous and Mesoporous Materials, 2020, 293, 109775.	2.2	41
84	FT-IR characterization and hydrolysis of PLA-PEG-PLA based copolyester hydrogels with short PLA segments and a cytocompatibility study. Journal of Polymer Science Part A, 2013, 51, 5163-5176.	2.5	40
85	Lowâ€Fouling Fluoropolymers for Bioconjugation and Inâ€Vivo Tracking. Angewandte Chemie - International Edition, 2020, 59, 4729-4735.	7.2	40
86	Configurational Assignments for Poly(methacrylonitrile) Using Double-Quantum-Filtered Phase-Sensitive COSY and Proton-Detected 1H-13C Shift-Correlated NMR Spectroscopies. Macromolecules, 1994, 27, 1830-1834.	2.2	39
87	NMR investigation of effect of dissolved salts on the thermoresponsive behavior of oligo(ethylene) Tj ETQq1 1 0.	784314 rg 2.5	BT Overlock
88	Anti-thrombogenic Surface Coatings for Extracorporeal Membrane Oxygenation: A Narrative Review. ACS Biomaterials Science and Engineering, 2021, 7, 4402-4419.	2.6	39
89	Laboratory wear testing of polyurethane elastomers. Wear, 1997, 208, 155-160.	1.5	38
90	Water diffusion into radiation crosslinked PVA–PVP network hydrogels. Radiation Physics and Chemistry, 2011, 80, 213-218.	1.4	38

#	Article	IF	CITATIONS
91	Conformation of Hydrophobically Modified Thermoresponsive Poly(OEGMA- <i>co</i> -TFEA) across the LCST Revealed by NMR and Molecular Dynamics Studies. Macromolecules, 2015, 48, 3310-3317.	2.2	38
92	Evaluation of Polymeric Nanomedicines Targeted to PSMA: Effect of Ligand on Targeting Efficiency. Biomacromolecules, 2015, 16, 3235-3247.	2.6	38
93	Effects of magnetic field strength and particle aggregation on relaxivity of ultra-small dual contrast iron oxide nanoparticles. Materials Research Express, 2017, 4, 116105.	0.8	38
94	Overcoming Surfactant-Induced Morphology Instability of Noncrosslinked Diblock Copolymer Nano-Objects Obtained by RAFT Emulsion Polymerization. ACS Macro Letters, 2018, 7, 159-165.	2.3	38
95	Gradient copolymers – Preparation, properties and practice. European Polymer Journal, 2019, 116, 394-414.	2.6	38
96	NMR Study of the Radiation-Induced Cross-Linking of Poly(tetrafluoroethylene-co-perfluoromethyl) Tj ETQq0 0 0 r	gBT/Over	loçk 10 Tf 5
97	N.m.r. imaging of the diffusion of water into poly(tetrahydrofurfuryl methacrylate-co-hydroxyethyl) Tj ETQq1 1 0.7	'84314 rgi 1.8	BŢ /Overloch
98	The radical homopolymerization of N -phenylmaleimide, N - n -hexylmaleimide and N -cyclohexylmaleimide in tetrahydrofuran. Polymer, 2001, 42, 4791-4802.	1.8	37
99	Amphiphilic Triblock Copolymers of Methoxy-poly(ethylene) Tj ETQq1 1 0.784314 rgBT /Overlock 10 Tf 50 427 Td Osteoblast Attachment and Growth. Biomacromolecules, 2009, 10, 95-104.	l (glycol)-< 2.6	i>b-poly 36
100	Chain scission resists for extreme ultraviolet lithography based on high performance polysulfone-containing polymers. Journal of Materials Chemistry, 2011, 21, 5629.	6.7	36
101	Importance of Thermally Induced Aggregation on <sup>19</sup> F Magnetic Resonance Imaging of Perfluoropolyether-Based Comb-Shaped Poly(2-oxazoline)s. Biomacromolecules, 2019, 20, 365-374.	2.6	36
102	Sustained-release ketamine-loaded nanoparticles fabricated by sequential nanoprecipitation. International Journal of Pharmaceutics, 2020, 581, 119291.	2.6	36
103	Emergence of Hexagonally Close-Packed Spheres in Linear Block Copolymer Melts. Journal of the American Chemical Society, 2021, 143, 14106-14114.	6.6	36
104	Organicâ^'Inorganic Poly(Methyl Methacrylate) Hybrids with Confined Polyhedral Oligosilsesquioxane Macromonomers. Chemistry of Materials, 2005, 17, 1027-1035.	3.2	35
105	Fluorinated Glycopolymers as Reduction-responsive <sup>19</sup> F MRI Agents for Targeted Imaging of Cancer. Biomacromolecules, 2019, 20, 2043-2050.	2.6	35
106	PFG-NMR Measurements of the Self-Diffusion Coefficients of Water in Equilibrium Poly(HEMA-co-THFMA) Hydrogels. Biomacromolecules, 2002, 3, 554-559.	2.6	34
107	High-Speed MAS 19F NMR Analysis of an Irradiated Fluoropolymer. Macromolecules, 2002, 35, 5544-5549.	2.2	34
108	pH Dependence of the Progression in NMRT2Relaxation Times in Post-mortem Muscle. Journal of Agricultural and Food Chemistry, 2003, 51, 4072-4078.	2.4	34

#	Article	IF	CITATIONS
109	Patterning of Tailored Polycarbonate Based Nonâ€Chemically Amplified Resists Using Extreme Ultraviolet Lithography. Macromolecular Rapid Communications, 2010, 31, 1449-1455.	2.0	34
110	Controlled synthesis of up-conversion luminescent Gd/Tm-MOFs for pH-responsive drug delivery and UCL/MRI dual-modal imaging. Dalton Transactions, 2018, 47, 11253-11263.	1.6	34
111	Recent Advances in the Development of Theranostic Nanoparticles for Cardiovascular Diseases. Nanotheranostics, 2021, 5, 499-514.	2.7	34
112	Cellulose nanocrystals reinforced highly stretchable thermal-sensitive hydrogel with ultra-high drug loading. Carbohydrate Polymers, 2021, 266, 118122.	5.1	33
113	A Reinvestigation of Low-Carnegieite by XRD, NMR, and TEM. Journal of Solid State Chemistry, 1993, 104, 59-73.	1.4	32
114	Development of wear-resistant thermoplastic polyurethanes by blending with poly(dimethyl siloxane). II. A packing model. Journal of Applied Polymer Science, 1997, 65, 939-950.	1.3	32
115	The copolymerization of N-vinyl-2-pyrrolidone with 2-hydroxyethyl methacrylate. Polymer Bulletin, 2002, 47, 421-427.	1.7	32
116	Conformation Transitions of Thermoresponsive Dendronized Polymers across the Lower Critical Solution Temperature. Macromolecules, 2016, 49, 900-908.	2.2	32
117	Bioconjugation and Fluorescence Labeling of Iron Oxide Nanoparticles Grafted with Bromomaleimide-Terminal Polymers. Biomacromolecules, 2018, 19, 4423-4429.	2.6	32
118	Hyperbranched polymers for molecular imaging: designing polymers for parahydrogen induced polarisation (PHIP). Chemical Communications, 2012, 48, 1583-1585.	2.2	31
119	Tuning of the Aggregation Behavior of Fluorinated Polymeric Nanoparticles for Improved Therapeutic Efficacy. ACS Nano, 2020, 14, 7425-7434.	7.3	31
120	Chitosan Nanococktails Containing Both Ceria and Superparamagnetic Iron Oxide Nanoparticles for Reactive Oxygen Species-Related Theranostics. ACS Applied Nano Materials, 2021, 4, 3604-3618.	2.4	31
121	A solid-state 13C-NMR study of crosslinking in polybutadiene by Î <sup>3</sup> radiation: Effect of microstructure and dose. Journal of Polymer Science Part A, 1992, 30, 185-195.	2.5	30
122	The crosslinking mechanism in gamma irradiation of polyarylsulfone: evidence for Y-links. Polymers for Advanced Technologies, 1998, 9, 45-51.	1.6	30
123	Influence of synthesis parameters on the formation of mesoporous SAPOs. Microporous and Mesoporous Materials, 2002, 55, 51-62.	2.2	30
124	PEG-Based Hyperbranched Polymer Theranostics: Optimizing Chemistries for Improved Bioconjugation. Macromolecules, 2014, 47, 5211-5219.	2.2	30
125	Elucidating the Impact of Molecular Structure on the <sup>19</sup> F NMR Dynamics and MRI Performance of Fluorinated Oligomers. ACS Macro Letters, 2018, 7, 921-926.	2.3	30
126	Multifunctional drug carrier on the basis of 3d–4f Fe/La-MOFs for drug delivery and dual-mode imaging. Journal of Materials Chemistry B, 2019, 7, 6612-6622.	2.9	30

#	Article	IF	CITATIONS
127	Proteins Conjugated with Sulfoxide-Containing Polymers Show Reduced Macrophage Cellular Uptake and Improved Pharmacokinetics. ACS Macro Letters, 2020, 9, 799-805.	2.3	30
128	Proton conduction mechanism and the stability of sol–gel titanium phosphates. Solid State Ionics, 2007, 177, 3389-3394.	1.3	29
129	The radiation degradation of a nanotube–polyimide nanocomposite. Polymer Degradation and Stability, 2008, 93, 169-175.	2.7	29
130	NMR as a probe of nanostructured domains in ionic liquids: Does domain segregation explain increased performance of free radical polymerisation?. Chemical Science, 2011, 2, 1810.	3.7	29
131	Molecular motion in nanocomposites of poly(ethylene oxide) and montmorillonite. Journal of Polymer Science, Part B: Polymer Physics, 2001, 39, 1678-1685.	2.4	28
132	Equilibrium Swelling Measurements of Network and Semicrystalline Polymers in Supercritical Carbon Dioxide Using High-Pressure NMR. Macromolecules, 2005, 38, 3731-3737.	2.2	28
133	Multiple Hydrogen-Bonded Complexes Based on 2-Ureido-4[1 <i>H</i> ]-pyrimidinone: A Theoretical Study. Journal of Physical Chemistry B, 2011, 115, 11053-11062.	1.2	28
134	Controlled polymerisation of lactide using an organo-catalyst in supercritical carbon dioxide. Green Chemistry, 2011, 13, 2032.	4.6	28
135	Effect of Solvent Quality on the Solution Properties of Assemblies of Partially Fluorinated Amphiphilic Diblock Copolymers. Macromolecules, 2012, 45, 8681-8690.	2.2	28
136	Multifunctional hyperbranched polymers for CT/ <sup>19</sup> F MRI bimodal molecular imaging. Polymer Chemistry, 2016, 7, 1059-1069.	1.9	28
137	Hydrogels with Lotus Leaf Topography: Investigating Surface Properties and Cell Adhesion. Langmuir, 2017, 33, 485-493.	1.6	28
138	3D shape change of multi-responsive hydrogels based on a light-programmed gradient in volume phase transition. Chemical Communications, 2018, 54, 10909-10912.	2.2	28
139	Molecular Cocrystals of Carboxylic Acids. XIV. The Crystal Structures of the Adducts of Pyrazine-2,3-dicarboxylic Acid With 4-Aminobenzoic Acid, 3-Hydroxypyridine and 3-Amino-1,2,4-triazole. Australian Journal of Chemistry, 1994, 47, 309.	0.5	27
140	NMR Imaging of Water Sorption into Poly(hydroxyethyl methacrylate-co-tetrahydrofurfuryl) Tj ETQq0 0 0 rgBT /C	)verlock 10	) Tf 50 222 T
141	Salt Diffusion and Distribution in Meat Studied by23Na Nuclear Magnetic Resonance Imaging and Relaxometry. Journal of Agricultural and Food Chemistry, 2005, 53, 7814-7818.	2.4	27
142	Hydrolytic degradation of POSS–PEG–lactide hybrid hydrogels. Polymer Degradation and Stability, 2011, 96, 123-130.	2.7	27
143	Ageingâ€induced solubility loss in milk protein concentrate powder: effect of protein conformational modifications and interactions with water. Journal of the Science of Food and Agriculture, 2011, 91, 2576-2581.	1.7	27
144	Comparative study of preclinical mouse models of high-grade glioma for nanomedicine research: the importance of reproducing blood-brain barrier heterogeneity. Theranostics, 2020, 10, 6361-6371.	4.6	27

#	Article	IF	CITATIONS
145	The radiation chemistry of poly(dimethyl-siloxane). Macromolecular Symposia, 2000, 156, 95-102.	0.4	26
146	The radiation crosslinking and scission of ethylene-propylene copolymers studied by solid-state nuclear magnetic resonance. British Polymer Journal, 1985, 17, 51-55.	0.7	25
147	Structural Characterisation of Kaolinite:NaCl Intercalate and its Derivatives. Clays and Clay Minerals, 1992, 40, 369-380.	0.6	25
148	Kinetics of enthalpy relaxation of milk protein concentrate powder upon ageing and its effect on solubility. Food Chemistry, 2012, 134, 1368-1373.	4.2	25
149	Behavior of Lamellar Forming Block Copolymers under Nanoconfinement: Implications for Topography Directed Self-Assembly of Sub-10 nm Structures. Macromolecules, 2014, 47, 276-283.	2.2	25
150	Functional polymers as metal-free magnetic resonance imaging contrast agents. Progress in Polymer Science, 2020, 108, 101286.	11.8	25
151	Rapid Generation of Block Copolymer Libraries Using Automated Chromatographic Separation. Journal of the American Chemical Society, 2020, 142, 9843-9849.	6.6	25
152	Inhibition of Amyloid Aggregation and Toxicity with Janus Iron Oxide Nanoparticles. Chemistry of Materials, 2021, 33, 6484-6500.	3.2	25
153	Influence of surface oxidation on the quantification of polypropylene microplastics by pyrolysis gas chromatography mass spectrometry. Science of the Total Environment, 2021, 796, 148835.	3.9	25
154	Molecular motions in poly(diethyl siloxane) studied by solid-state29Si NMR. Colloid and Polymer Science, 1989, 267, 681-686.	1.0	24
155	Water diffusion in hydroxyethyl methacrylate (HEMA)-based hydrogels formed by γ-radiolysis. Polymer International, 1999, 48, 1046-1052.	1.6	24
156	Effect of phosphate functional groups on the calcification capacity of acrylic hydrogels. Acta Biomaterialia, 2007, 3, 95-102.	4.1	24
157	Structure and Molecular Mobility of Soy Glycinin in the Solid State. Biomacromolecules, 2008, 9, 2937-2946.	2.6	24
158	Facile Synthesis of Largeâ€Pore Bicontinuous Cubic Mesoporous Silica Nanoparticles for Intracellular Gene Delivery. ChemNanoMat, 2016, 2, 220-225.	1.5	24
159	Novel Polymeric Bioerodable Microparticles for Prolonged-Release Intrathecal Delivery of Analgesic Agents for Relief of Intractable Cancer-Related Pain. Journal of Pharmaceutical Sciences, 2015, 104, 2334-2344.	1.6	23
160	Multifunctional Magnetized Porous Silica Covered with Poly(2-dimethylaminoethyl methacrylate) for pH Controllable Drug Release and Magnetic Resonance Imaging. ACS Applied Nano Materials, 2018, 1, 5027-5034.	2.4	23
161	Observation by 13C n.m.r. of H-crosslinks and methyl end groups due to main-chain scission in ethylene-propylene copolymers after Î <sup>3</sup> -irradiation. Polymer, 1992, 33, 62-67.	1.8	22
162	Versatile synthetic approach to reversible crosslinked polystyrene networks via RAFT polymerization. Journal of Polymer Science Part A, 2007, 45, 4150-4153.	2.5	22

#	Article	IF	CITATIONS
163	"Click―PNIPAAm hydrogels – a comprehensive study of structure and properties. Polymer Chemistry, 2013, 4, 4788.	1.9	22
164	Lowâ€Fouling Fluoropolymers for Bioconjugation and Inâ€Vivo Tracking. Angewandte Chemie, 2020, 132, 4759-4765.	1.6	22
165	Cross-Linking of PFA by Electron Beam Irradiation. Macromolecules, 2003, 36, 7138-7142.	2.2	21
166	Visualization of drip channels in meat using NMR microimaging. Meat Science, 2004, 68, 667-670.	2.7	21
167	Experimental Calcification of HEMA-Based Hydrogels in the Presence of Albumin and a Comparison to the in Vivo Calcification. Biomacromolecules, 2006, 7, 1758-1765.	2.6	21
168	Synthesis of aliphatic polycarbonates with a tuneable thermal response. Polymer Chemistry, 2017, 8, 5082-5090.	1.9	21
169	Composition and Crystallinity Effects in the Degradation of Ethylene-Propylene Copolymers by γ-Radiation. Journal of Macromolecular Science - Pure and Applied Chemistry, 1992, 29, 1-10.	1.2	20
170	Measurement of Radical Yields To Assess Radiation Resistance in Engineering Thermoplastics. Advances in Chemistry Series, 1996, , 637-649.	0.6	20
171	The radiation chemistry of the copolymer of tetrafluoroethylene with 2,2-bis(trifluoromethyl)-4,5-difluoro-1,3-dioxole. Polymer Degradation and Stability, 1999, 63, 95-101.	2.7	20
172	New Structure Formation on $\hat{I}^3$ -irradiation of Poly(chlorotrifluoroethylene). Radiation Physics and Chemistry, 2003, 67, 729-736.	1.4	20
173	An Investigation of the Thermal and Tensile Properties of PFA Following Î <sup>3</sup> -Radiolysis. Macromolecules, 2003, 36, 7132-7137.	2.2	19
174	Mechanism of 157 nm Photodegradation of Poly[4,5-difluoro-2,2- bis(trifluoromethyl)-1,3-dioxole-co-tetrafluoroethylene] (Teflon AF). Macromolecules, 2007, 40, 8954-8961.	2.2	19
175	Processing of nanocomposite foams in supercritical carbon dioxide. Part I: Effect of surfactant. Polymer, 2010, 51, 3436-3444.	1.8	19
176	Controlled release of ketorolac through nanocomposite films of hydrogel and LDH nanoparticles. Journal of Nanoparticle Research, 2011, 13, 1253-1264.	0.8	19
177	Aqueous developable dual switching photoresists for nanolithography. Journal of Polymer Science Part A, 2012, 50, 4255-4265.	2.5	19
178	Using Directed Self Assembly of Block Copolymer Nanostructures to Modulate Nanoscale Surface Roughness: Towards a Novel Lithographic Process. Advanced Functional Materials, 2013, 23, 173-183.	7.8	19
179	Coordination complexes as molecular glue for immobilization of antibodies on cyclic olefin copolymer surfaces. Analytical Biochemistry, 2014, 456, 6-13.	1.1	19
180	Change in molecular structure and dynamics of protein in milk protein concentrate powder upon ageing by solid-state carbon NMR. Food Hydrocolloids, 2015, 44, 66-70.	5.6	19

#	Article	IF	CITATIONS
181	Fluorinated POSS tar Polymers for <sup>19</sup> F MRI. Macromolecular Chemistry and Physics, 2016, 217, 2262-2274.	1.1	19
182	Ultrasound-triggered release from metal shell microcapsules. Journal of Colloid and Interface Science, 2019, 554, 444-452.	5.0	19
183	Red fluorescent AuNDs with conjugation of cholera toxin subunit B (CTB) for extended-distance retro-nerve transporting and long-time neural tracing. Acta Biomaterialia, 2020, 102, 394-402.	4.1	19
184	An ESR study of the radiation chemistry of poly (tetrafluoroethylene-co-hexafluoropropylene) at 77 and 300 K. Radiation Physics and Chemistry, 2000, 59, 295-302.	1.4	18
185	Investigation of spontaneous microemulsion formation in supercritical carbon dioxide using high-pressure NMR. Journal of Supercritical Fluids, 2006, 38, 111-118.	1.6	18
186	Comprehensive Characterization of Grafted Expanded Poly(tetrafluoroethylene) for Medical Applications. Langmuir, 2010, 26, 15409-15417.	1.6	18
187	Extreme ultraviolet (EUV) degradation of poly(olefin sulfone)s: Towards applications as EUV photoresists. Radiation Physics and Chemistry, 2011, 80, 236-241.	1.4	18
188	Bioinspired Core–Shell Nanoparticles for Hydrophobic Drug Delivery. Angewandte Chemie, 2019, 131, 14495-14502.	1.6	18
189	Magnetic and Photocatalytic Curcumin Bound Carbon Nitride Nanohybrids for Enhanced Glioma Cell Death. ACS Biomaterials Science and Engineering, 2019, 5, 6590-6601.	2.6	18
190	Amphiphilic Perfluoropolyether Copolymers for the Effective Removal of Polyfluoroalkyl Substances from Aqueous Environments. Macromolecules, 2021, 54, 3447-3457.	2.2	18
191	Facile bioinspired synthesis of iron oxide encapsulating silica nanocapsules. Journal of Colloid and Interface Science, 2021, 601, 78-84.	5.0	18
192	Determination of residual unsaturation in highly crosslinked, dough-moulded poly(methyl) Tj ETQq0 0 0 rgBT /O	verlock 10 1.3	Tf 50 307 Td 17
193	Water sorption by poly(tetrahydrofurfuryl methacrylate-co-2-hydroxyethyl methacrylate). I. A mass-uptake study. Journal of Polymer Science, Part B: Polymer Physics, 2000, 38, 1939-1946.	2.4	17
194	NMR Imaging of the Diffusion of Water at 310 K into Semi-IPNs of PEM and Poly(HEMA-co-THFMA) with and without Chlorhexidine Diacetate. Biomacromolecules, 2004, 5, 1405-1411.	2.6	17
195	Determination of Domain Sizes in Blends of Poly(ethylene) and Poly(styrene) Formed in the Presence of Supercritical Carbon Dioxide. Macromolecules, 2004, 37, 6019-6026.	2.2	17
196	Photo-initiated thiol-ene "click―hydrogels from RAFT-synthesized poly( <i>N</i> -isopropylacrylamide). Journal of Polymer Science Part A, 2013, 51, 4626-4636.	2.5	17
197	Self-assembled magnetic luminescent hybrid micelles containing rare earth Eu for dual-modality MR and optical imaging. Journal of Materials Chemistry B, 2014, 2, 546-555.	2.9	17
198	Aqueous solution behaviour of novel water-soluble amphiphilic copolymers with elevated hydrophobic unit content. Polymer Chemistry, 2017, 8, 4114-4123.	1.9	17

#	Article	IF	CITATIONS
199	Engineering chitosan nano-cocktail containing iron oxide and ceria: A two-in-one approach for treatment of inflammatory diseases and tracking of material delivery. Materials Science and Engineering C, 2021, 131, 112477.	3.8	17
200	Revealing the Molecular-Level Interactions between Cationic Fluorinated Polymer Sorbents and the Major PFAS Pollutant PFOA. Macromolecules, 2022, 55, 1077-1087.	2.2	17
201	Solid-State 31P N.M.R. and Crystal Structure of Binuclear Di-μ-chloro-bis[(4-methylpyridine)(triphenyl-phosphine)copper(I)]. Australian Journal of Chemistry, 1991, 44, 729.	0.5	16
202	The effect of field inhomogeneities and molecular diffusion on the NMR transverse relaxation behaviour of polymer melts. Polymer, 1995, 36, 2159-2164.	1.8	16
203	Investigation of High-Temperature Radiation Effects on Poly(methyl methacrylate) of Specific Tacticity. Macromolecules, 1995, 28, 3681-3691.	2.2	16
204	Study of the calcification of PHEMA hydrogels using a two compartment permeation cell. Journal of Molecular Structure, 2005, 739, 199-206.	1.8	16
205	Computer simulation and preparation of molecularly imprinted polymer membranes with chlorogenic acid as template. Polymer International, 2011, 60, 592-598.	1.6	16
206	A study of the swelling and model protein release behaviours of radiation-formed poly(N-vinyl) Tj ETQq0 0 0 rgB	Г /Qverloct 1.4	۶ 10 Tf 50 46 16
207	Journey to the Market: The Evolution of Biodegradable Drug Delivery Systems. Applied Sciences (Switzerland), 2022, 12, 935.	1.3	16
208	Thermoresponsive Supramolecular Assemblies from Dendronized Amphiphiles To Form Fluorescent Spheres with Tunable Chirality. ACS Nano, 2021, 15, 20067-20078.	7.3	16
209	<sup>1</sup> H spinâ€lattice relaxation and observation of interfacial material in solid polyethylenes. Makromolekulare Chemie Macromolecular Symposia, 1990, 34, 161-170.	0.6	15
210	Characterization of the Acidic Properties of Mesoporous Aluminosilicates Synthesized from Leached Saponite with Additional Aluminum Incorporation. Journal of Physical Chemistry B, 2003, 107, 8599-8606.	1.2	15
211	Physicochemical and Structural Characterization of Mesoporous Aluminosilicates Synthesized from Leached Saponite with Additional Aluminum Incorporation. Chemistry of Materials, 2003, 15, 4863-4873.	3.2	15
212	The use of simultaneous 1H & 31P magic angle spinning nuclear magnetic resonance measurements to characterize energy metabolism during the conversion of muscle to meat. International Journal of Food Science and Technology, 2004, 39, 661-670.	1.3	15
919	In-vitro study of the spontaneous calcification of PHEMA-based hydrogels in simulated body fluid.	17	15

213	Journal of Materials Science: Materials in Medicine, 2006, 17, 1245-1254.	1.7	10
214	Enhanced human bone marrow stromal cell affinity for modified poly(l-lactide) surfaces by the upregulation of adhesion molecular genes. Biomaterials, 2009, 30, 6903-6911.	5.7	15
215	The potential for remodelling the tumour vasculature in glioblastoma. Advanced Drug Delivery Reviews, 2018, 136-137, 49-61.	6.6	15

<sup>216</sup>An investigation into the synthesis of polycarbazole squaraine derivatives. Polymer Bulletin, 1997, 38,<br/>493-499.1.714

#	Article	IF	CITATIONS
217	NMR Imaging of the Diffusion of Water at 37 °C into Poly(2-hydroxyethyl methacrylate) Containing Aspirin or Vitamin B12. Biomacromolecules, 2004, 5, 971-976.	2.6	14
218	Novel high-index resists for 193-nm immersion lithography and beyond. , 2007, 6519, 110.		14
219	Preferential interactions of calcium ions in poly(2-hydroxyethyl methacrylate) hydrogels. Journal of Materials Science: Materials in Medicine, 2007, 18, 1141-1149.	1.7	14
220	F2 excimer laser (157nm) radiation modification and surface ablation of PHEMA hydrogels and the effects on bioactivity: Surface attachment and proliferation of human corneal epithelial cells. Radiation Physics and Chemistry, 2011, 80, 219-229.	1.4	14
221	Polysulfone based non-CA resists for 193nm immersion lithography: Effect of increasing polymer absorbance on sensitivity. Radiation Physics and Chemistry, 2011, 80, 242-247.	1.4	14
222	The influence of composition on the physical properties of PLA-PEG-PLA-co-Boltorn based polyester hydrogels and their biological performance. Journal of Materials Chemistry, 2012, 22, 6994.	6.7	14
223	Polymeric <scp>siRNA</scp> delivery vectors: knocking down cancers with polymericâ€based gene delivery systems. Journal of Chemical Technology and Biotechnology, 2015, 90, 1196-1208.	1.6	14
224	Functional magnetic porous silica for <i>T</i> <sub>1</sub> – <i>T</i> <sub>2</sub> dual-modal magnetic resonance imaging and pH-responsive drug delivery of basic drugs. Nanotechnology, 2016, 27, 485702.	1.3	14
225	Self-confirming molecular imaging of activated platelets via iron oxide nanoparticles displaying unique dual MRI contrast. Atherosclerosis, 2017, 263, e146.	0.4	14
226	Controllable synthesis of a novel magnetic core–shell nanoparticle for dual-modal imaging and pH-responsive drug delivery. Nanotechnology, 2017, 28, 495101.	1.3	14
227	Physisorption of Poly(ethylene glycol) on Inorganic Nanoparticles. ACS Nano, 2022, 16, 6634-6645.	7.3	14
228	One-step nanoarchitectonics of a multiple functional hydrogel based on cellulose nanocrystals for effective tumor therapy. Nano Research, 2022, 15, 8636-8647.	5.8	14
229	A comparative study of the effects of UV- and γ-radiation on copolymers of acrylonitrile/butadiene. Polymer International, 1999, 48, 985-992.	1.6	13
230	Water sorption into poly[(2-hydroxyethyl methacrylate)-co-(1-vinyl-2-pyrrolidone)]at 310 K. Polymer International, 2003, 52, 1740-1748.	1.6	13
231	Postsynthesis Stabilization of Free-standing Mesoporous Silica Films. Langmuir, 2004, 20, 2908-2914.	1.6	13
232	High-RI resist polymers for 193 nm immersion lithography. , 2005, 5753, 827.		13
233	The hydration of paper studied with solid-state magnetisation-exchange 1H NMR spectroscopy. Holzforschung, 2006, 60, 409-416.	0.9	13
234	Development of polymers for non-CAR resists for EUV lithography. , 2009, , .		13

#	Article	IF	CITATIONS
235	Synthesis of a new hyperbranched, vinyl macromonomer through the use of click chemistry: Synthesis and characterization of copolymer hydrogels with PEG diacrylate. Journal of Polymer Science Part A, 2012, 50, 1143-1157.	2.5	13
236	Reactivity Ratios and Sequence Distribution Characterization by Quantitative <sup>13</sup> C NMR for RAFT Synthesis of Styreneâ€Acrylonitrile Copolymers. Journal of Polymer Science Part A, 2017, 55, 919-927.	2.5	13
237	Sustained-Release Hydromorphone Microparticles Produced by Supercritical Fluid Polymer Encapsulation. Journal of Pharmaceutical Sciences, 2019, 108, 811-814.	1.6	13
238	MR-guided focused ultrasound increases antibody delivery to nonenhancing high-grade glioma. Neuro-Oncology Advances, 2020, 2, vdaa030.	0.4	13
239	NMR imaging of the diffusion of water at 310 K into poly[(2-hydroxyethyl) Tj ETQq1 1 0.784314 rgBT /Overlock International, 2005, 54, 267-273.	10 Tf 50 5 1.6	587 Td (metha 12
240	XPS and19F NMR Study of the Photodegradation at 157 nm of Photolithographic-Grade Teflon AF Thin Films. Macromolecules, 2005, 38, 4050-4053.	2.2	12
241	Novel Supramolecular Hydrogels as Artificial Vitreous Substitutes. Macromolecular Symposia, 2010, 296, 229-232.	0.4	12
242	Sodium-Ion Storage Mechanism in Triquinoxalinylene and a Strategy for Improving Electrode Stability. Energy & Fuels, 2020, 34, 5099-5105.	2.5	12
243	Miscibility Studies in Blends of Poly(methyl methacrylate) with Poly(styrene-co-methacrylonitrile) Using Solid-State NMR and Fluorescence Spectroscopy. Macromolecules, 1994, 27, 5912-5918.	2.2	11
244	Synthesis of high-refractive index sulfur containing polymers for 193-nm immersion lithography; a progress report. , 2006, 6153, 172.		11
245	Tensile properties and in vitro degradation of P(TMC-co-LLA) elastomers. Journal of Materials Chemistry B, 2015, 3, 4406-4416.	2.9	11
246	Cyclotriphosphazene, a scaffold for 19 F MRI contrast agents. Tetrahedron Letters, 2018, 59, 521-523.	0.7	11
247	Spatial arrangement of block copolymer nanopatterns using a photoactive homopolymer substrate. Nanoscale Advances, 2019, 1, 3078-3085.	2.2	11
248	Evaluating the effect of synthesis, isolation, and characterisation variables on reported particle size and dispersity of drug loaded PLGA nanoparticles. Materials Advances, 2021, 2, 5657-5671.	2.6	11
249	Microconfinement from Dendronized Chitosan Oligosaccharides for Mild Synthesis of Silver Nanoparticles. ACS Applied Nano Materials, 2022, 5, 4350-4359.	2.4	11
250	The copolymerisation of tetrahydrofurfuryl methacrylate and methyl methacrylate. Polymer Gels and Networks, 1996, 4, 253-267.	0.6	10
251	Thermal and mechanical properties of radiation crosslinked poly(tetrafluoroethylene-co-perfluoromethyl vinyl ether). Radiation Physics and Chemistry, 1998, 53, 657-667.	1.4	10
252	A study of the copolymerization of hydroxyethyl methacrylate and tetrahydrofurfuryl methacrylate. Journal of Polymer Science Part A, 1999, 37, 3730-3737.	2.5	10

#	Article	IF	CITATIONS
253	The radiation chemistry of ultem at 77K as revealed by ESR spectroscopy. Radiation Physics and Chemistry, 2002, 64, 299-308.	1.4	10
254	Chain scission and branching in irradiated poly(tetrafluoroethylene-co-hexafluoropropylene). Polymer International, 2003, 52, 1725-1733.	1.6	10
255	Towards identifying the new structures formed on the Î <sup>3</sup> -radiolysis of Ultem. Radiation Physics and Chemistry, 2004, 69, 65-77.	1.4	10
256	The rational design of polymeric EUV resist materials by QSPR modelling. , 2007, , .		10
257	Surface Plasma Modification of LLDPE for Biomedical Applications. Polymer-Plastics Technology and Engineering, 2009, 49, 1-7.	1.9	10
258	Molecular Water Motions of Skim Milk Powder Solutions during Acidification Studied by <sup>17</sup> 0 and <sup>1</sup> H Nuclear Magnetic Resonance and Rheology. Journal of Agricultural and Food Chemistry, 2011, 59, 10097-10103.	2.4	10
259	The role of residual Cu(ii) from click-chemistry in the catalyzed hydrolysis of Boltorn polyester-based hydrogels. Soft Matter, 2012, 8, 435-445.	1.2	10
260	Synthesis, swelling, degradation and cytocompatibility of crosslinked PLLA-PEG-PLLA networks with short PLLA blocks. European Polymer Journal, 2016, 84, 448-464.	2.6	10
261	Electrospinning and mechanical properties of P(TMC-co-LLA) elastomers. Journal of Materials Chemistry B, 2017, 5, 2263-2272.	2.9	10
262	Vitamin B12 Release from P(HEMA-co-THFMA) in Water and SBF: A Model Drug Release Study. Australian Journal of Chemistry, 2005, 58, 451.	0.5	10
263	NMR Studies of Cross linked Polymers. Annual Reports on NMR Spectroscopy, 1997, , 105-183.	0.7	9
264	Effect of temperature on the γ-radiolysis of poly(tetrafluoroethylene-co-perfluoromethyl vinyl ether). Radiation Physics and Chemistry, 1998, 53, 611-621.	1.4	9
265	Absorption of low molecular weight penetrants by a thermoplastic polyimide. Polymer, 2000, 41, 7263-7271.	1.8	9
266	Study of wet porous filtration. Separation and Purification Technology, 2003, 30, 129-137.	3.9	9
267	The States, Diffusion, and Concentration Distribution of Water in Radiationâ€Formed PVA/PVP Hydrogels. Soft Materials, 2004, 2, 195-212.	0.8	9
268	A Study of the Swelling of Copolymers of NIPAM and DMA with Water by NMR Imaging. Applied Magnetic Resonance, 2007, 32, 51-62.	0.6	9
269	Non-CA resists for 193 nm immersion lithography: effects of chemical structure on sensitivity. Proceedings of SPIE, 2009, , .	0.8	9
270	Photochemistry of Iowâ€density polyethylene–montmorillonite composites. Journal of Applied Polymer Science, 2009, 112, 381-389.	1.3	9

#	Article	IF	CITATIONS
271	Polycarbonate based nonchemically amplified photoresists for extreme ultraviolet lithography. Proceedings of SPIE, 2010, , .	0.8	9
272	Development of Injectable Biodegradable Multiâ€Arms PEGâ€Based Hydrogels: Swelling and Degradation Investigations. Macromolecular Symposia, 2010, 296, 233-237.	0.4	9
273	Electrochemical DNA biosensor based on ILâ€modified MWNTs electrode prepared by radiationâ€induced graft polymerization. Journal of Applied Polymer Science, 2012, 126, E28.	1.3	9
274	Click functionalization of methacrylate-based hydrogels and their cellular response. Journal of Polymer Science Part A, 2014, 52, 1781-1789.	2.5	9
275	A two-step synthesis for preparing metal microcapsules with a biodegradable polymer substrate. Journal of Materials Chemistry B, 2018, 6, 2151-2158.	2.9	9
276	Use of Microfluidics to Fabricate Bioerodable Lipid Hybrid Nanoparticles Containing Hydromorphone or Ketamine for the Relief of Intractable Pain. Pharmaceutical Research, 2020, 37, 211.	1.7	9
277	Investigation of heparin-loaded poly(ethylene glycol)-based hydrogels as anti-thrombogenic surface coatings for extracorporeal membrane oxygenation. Journal of Materials Chemistry B, 2022, 10, 4974-4983.	2.9	9
278	Photolysis of acetone at 100 – 170 K: an electron spin resonance study of radical formation and decay in the solid state. Journal of Photochemistry and Photobiology, 1984, 26, 255-267.	0.6	8
279	A technique for the quantitative measurements of signal intensities in cellulose-based transformer insulators by13C CPMAS NMR. Cellulose, 1994, 1, 237-247.	2.4	8
280	Radiation chemistry of poly(tetrafluoroethylene-co-perfluoromethyl vinyl ether): Effects of oxygen and crystallinity. Journal of Applied Polymer Science, 1999, 73, 807-812.	1.3	8
281	Synthesis, thermal and radiation sensitivities of some linear aromatic polyesters. Polymer International, 1999, 48, 971-979.	1.6	8
282	A study of the radiation chemistry of poly(chlorotrifluoroethylene) by ESR spectroscopy. Radiation Physics and Chemistry, 2003, 68, 857-864.	1.4	8
283	Water diffusion in methacrylate based copolymer hydrogels of 2-hydroxyethyl methacrylate. Macromolecular Symposia, 2004, 207, 111-124.	0.4	8
284	NMR Microscopy: A Tool for Measuring Monomer Diffusion in Supercritical CO2. Macromolecular Chemistry and Physics, 2006, 207, 1539-1545.	1.1	8
285	Graft copolymerization of methoxyacrylethyl phosphate onto expanded poly(tetrafluoroethylene) facial membranes. Journal of Applied Polymer Science, 2010, 117, 3331-3339.	1.3	8
286	Degradable Hydrogels for Tissue Engineering – Part I: Synthesis by RAFT Polymerization and Characterization of PHEMA Containing Enzymatically Degradable Crosslinks. Journal of Biomimetics, Biomaterials, and Tissue Engineering, 2010, 6, 67-85.	0.7	8
287	The influence of casting parameters on the surface morphology of PS―b â€P4VP honeycomb films. Journal of Polymer Science Part A, 2016, 54, 3721-3732.	2.5	8
288	Formulation of Bioerodible Ketamine Microparticles as an Analgesic Adjuvant Treatment Produced by Supercritical Fluid Polymer Encapsulation. Pharmaceutics, 2018, 10, 264.	2.0	8

#	Article	IF	CITATIONS
289	The Impact of Polymer Size and Cleavability on the Intravenous Pharmacokinetics of PEG-Based Hyperbranched Polymers in Rats. Nanomaterials, 2020, 10, 2452.	1.9	8
290	Synthesis of 4-acetoxystyrene – t-butyl acrylate statistical, block and gradient copolymers, and the effect of the structure of copolymers on their properties. European Polymer Journal, 2020, 134, 109772.	2.6	8
291	A13C-n.m.r. study of radiation-induced racemization in isotactic polypropylene. British Polymer Journal, 1987, 19, 223-226.	0.7	7
292	Molecular Cocrystals of Carboxylic Acids. XVII. Spectral Characterization of the Adducts of Triphenylphosphine Oxide With Substituted Phenoxyacetic Acids and the Crystal Structure of the 1 : 1 Adduct With (4-Chloro-2-methylphenoxy)acetic Acid. Australian Journal of Chemistry, 1994, 47, 1401.	0.5	7
293	1H NMR studies of the radiation-induced crosslinking of poly(ethylene). Radiation Physics and Chemistry, 1996, 48, 601-604.	1.4	7
294	Title is missing!. Biotechnology Letters, 2002, 24, 521-525.	1.1	7
295	An Investigation of the Nitroxide-Mediated Preirradiation Grafting of Styrene onto PFA. Macromolecules, 2004, 37, 360-366.	2.2	7
296	DOSY NMR Studies of Chemical Exchange Behavior of Poly(2-hydroxyethyl methacrylate). Macromolecules, 2006, 39, 3878-3889.	2.2	7
297	Rational Design of High-RI Resists for 193nm Immersion Lithography. Journal of Photopolymer Science and Technology = [Fotoporima Konwakai Shi], 2007, 20, 665-671.	0.1	7
298	Development of an operational high refractive index resist for 193nm immersion lithography. , 2008, , .		7
299	Non-chemically amplified resists for 193-nm immersion lithography: influence of absorbance on performance. Proceedings of SPIE, 2010, , .	0.8	7
300	Control through monomer placement of surface properties and morphology of fluoromethacrylate copolymers. Journal of Polymer Science Part A, 2015, 53, 2633-2641.	2.5	7
301	Terpolymerization of Styrenic Photoresist Polymers: Effect of RAFT Polymerization on the Compositional Heterogeneity. Macromolecules, 2015, 48, 3438-3448.	2.2	7
302	Healing surface roughness of lithographic nanopatterns through sub-10 nm aqueous-dispersible polymeric particles with excellent dry etch durability. Molecular Systems Design and Engineering, 2018, 3, 627-635.	1.7	7
303	Bioerodable Ketamine-Loaded Microparticles Fabricated Using Dissolvable Hydrogel Template Technology. Journal of Pharmaceutical Sciences, 2019, 108, 1220-1226.	1.6	7
304	Development of a hyperbranched polymer-based methotrexate nanomedicine for rheumatoid arthritis. Acta Biomaterialia, 2022, 142, 298-307.	4.1	7
305	Thermal and Radiation Curing of Phenylethynyl Terminated Macromers. High Performance Polymers, 1999, 11, 453-465.	0.8	6
306	NMR studies of the radiation modification of polymers. Annual Reports on NMR Spectroscopy, 2002, 46, 1-35.	0.7	6

#	Article	IF	CITATIONS
307	NMR characterization of blends of poly(hydroxybutyrate-co-hydroxyvalerate) with poly(vinyl) Tj ETQq1 1 0.78431	4 [gBT /O\	verlock 10 Tf
308	A study of the radiation degradation of styrene/alkane and ?-methylstyrene/alkane copolymers. Polymer International, 2003, 52, 1711-1718.	1.6	6
309	Investigation of the Vapor-Phase Grafting of Styrene onto PFA. Macromolecules, 2003, 36, 8276-8281.	2.2	6
310	Antimicrobial anilinium polymers: The properties of poly( N , N â€dimethylaminophenylene) Tj ETQq0 0 0 rgBT /Ov	verlock 10 2.5	Tf 50 622 To
311	"Dual-Key-and-Lock―dual drug carrier for dual mode imaging guided chemo-photothermal therapy. Biomaterials Science, 2020, 8, 6212-6224.	2.6	6
312	Ultrasmall Red Fluorescent Gold Nanoclusters for Highly Biocompatible and Longâ€Time Nerve Imaging. Particle and Particle Systems Characterization, 2021, 38, 2100001.	1.2	6
313	Dendronized polydiacetylenes via photo-polymerization of supramolecular assemblies showing thermally tunable chirality. Chemical Communications, 2021, 57, 12780-12783.	2.2	6
314	The high resolution 13C NMR spectrum of poly(N,N?-bis(phenoxyphenyl) pyromellitimide), (Kapton). Polymer Bulletin, 1984, 12, 319-325.	1.7	5
315	The UV photolysis of N-acetyl amino acids studies by ESR as models for biological polypeptides. Polymer Degradation and Stability, 1986, 7, 13-25.	0.5	5
316	Mass uptake study of the diffusion of water and SBF into poly(2-hydroxyethyl) Tj ETQq0 0 0 rgBT /Overlock 10 Tf Biomaterials Science, Polymer Edition, 2005, 16, 1047-1061.	50 387 To 1.9	l (methacryla 5
317	The Structure of Polymer Networks. , 2008, , 583-589.		5
318	Mineralization of radiation-crosslinked polyvinyl alcohol/polyvinyl pyrrolidone hydrogels. Journal of Biomedical Materials Research - Part A, 2007, 83A, 354-361.	2.1	5
319	Magnetizationâ€prepared NMR imaging of water penetration into poly(vinyl) Tj ETQq1 1 0.784314 rgBT /Overloc	k 10 Tf 50 1.6	262 Td (alc
320	High-pressure real-time 129Xe NMR: monitoring of surfactant conformation during the self-assembly of reverse micelles in supercritical carbon dioxide. Chemical Communications, 2010, 46, 2850.	2.2	5
321	EUVL compatible LER solutions using functional block copolymers. Proceedings of SPIE, 2012, , .	0.8	5
322	Photo/Thermal Dual Responses in Aqueous-Soluble Copolymers Containing 1-Naphthyl Methacrylate. Macromolecules, 2021, 54, 4860-4870.	2.2	5
323	Tuning the thermoresponsive properties of PEG-based fluorinated polymers and stimuli responsive drug release for switchable <sup>19</sup> F magnetic resonance imaging. Polymer Chemistry, 2021, 12, 5438-5448.	1.9	5
324	Molecular Cocrystals of Carboxylic Acids. XXVII An Investigation into the Use of Triphenylphosphine Oxide Cocrystals for Non-Linear Optics: the Crystal Structure of the Adduct of Triphenylphosphine Oxide with N-Methylpyrrole-2-carboxylic Acid. Australian Journal of Chemistry, 1997, 50, 1191.	0.5	5

#	Article	IF	CITATIONS
325	Supramolecular Chiral Assembly of Symmetric Molecules with an Extended Conjugated Core. ACS Applied Materials & Interfaces, 2022, 14, 33734-33745.	4.0	5
326	Radiation degradation of linear low density polyethylene: Determination of lamellae thickness, crystallinity and crosslinking by solid-state 13C NMR and DSC. International Journal of Radiation Applications and Instrumentation Nuclear Tracks and Radiation Measurements, 1992, 39, 209-214.	0.0	4
327	G -Values for Scission and Crosslinking on γ — Radiolysis of Ultem at 303 K. High Performance Polymers, 2003, 15, 259-267.	0.8	4
328	The Effect of Synthetic Conditions on the Free Volume of Poly(2-hydroxyethyl methacrylate) as Studied by <sup>1</sup> H NMR, <sup>129</sup> Xe NMR, and Position Annihilation Spectroscopy. ACS Symposium Series, 2007, , 391-409.	0.5	4
329	Electron beam induced freezing of positive tone, EUV resists for directed self assembly applications. , 2011, , .		4
330	An electron spin resonance study of free radical reactions in gamma-irradiated N-acetyl-L-alanine. Radiation Physics and Chemistry (1977), 1985, 26, 191-196.	0.4	3
331	Polymerization of diglycidyl ether of bisphenol A/ diaminodiphenyl sulfone epoxy resins using radio frequency fields. Journal of Applied Polymer Science, 1999, 74, 2917.	1.3	3
332	Photodegradation of some lowâ€density polyethylene–montmorillonite nanocomposites containing an oligomeric compatibilizer. Journal of Applied Polymer Science, 2014, 131, .	1.3	3
333	Spectral normalisation by error minimisation for prediction of conversion in solvent-free catalytic chain transfer polymerisations. RSC Advances, 2016, 6, 69484-69491.	1.7	3
334	Synthesis and post-polymerisation ligations of PEC-based hyperbranched polymers for RNA conjugation via reversible disulfide linkage. Macromolecular Research, 2017, 25, 599-614.	1.0	3
335	Moisture-activated dynamics on crystallite surfaces in cellulose. Colloid and Polymer Science, 2019, 297, 521-527.	1.0	3
336	Sustained release ketamine-loaded porous silicon-PLGA microparticles prepared by an optimized supercritical CO2 process. Drug Delivery and Translational Research, 2021, , 1.	3.0	3
337	Optimisation of a Microfluidic Method for the Delivery of a Small Peptide. Pharmaceutics, 2021, 13, 1505.	2.0	3
338	Deposition of non-porous calcium phosphate shells onto liquid filled microcapsules. Journal of Colloid and Interface Science, 2022, 609, 575-583.	5.0	3
339	Radiation Degradation of Elastomers. Journal of Macromolecular Science - Pure and Applied Chemistry, 1993, 30, 633-644.	1.2	2
340	Recent developments in the radiation chemistry of elastomers. Macromolecular Symposia, 1995, 98, 689-699.	0.4	2
341	Novel Synthetic Bio-Mimic Polymers for Cell Delivery. Advanced Materials Research, 0, 32, 215-222.	0.3	2
342	Effect of Molecular Architecture on the Performance of <sup>19</sup> F NMR Imaging Agents. ACS Symposium Series, 2011, , 459-472.	0.5	2

#	Article	IF	CITATIONS
343	Templating core–shell particles using metal ion-chelating biosurfactants. Particuology, 2022, 64, 145-152.	2.0	2
344	Photolysis of poly(amino acid)s at 77K: An ESR study. Polymer Degradation and Stability, 1985, 10, 15-23.	2.7	1
345	Studies of the copolymerisation of acrylic acid withn-butyl vinyl ether. Polymer International, 2009, 58, 348-353.	1.6	1
346	Degradable Hydrogels for Tissue Engineering - Part II: Responses of Fibroblasts and Macrophages to Linear PHEMA. Journal of Biomimetics, Biomaterials, and Tissue Engineering, 2010, 8, 91-104.	0.7	1
347	Sensitive polysulfone based chain scissioning resists for 193nm lithography. , 2011, , .		1
348	Healing LER using directed self assembly: treatment of EUVL resists with aqueous solutions of block copolymers. Proceedings of SPIE, 2013, , .	0.8	1
349	Effect of changes in the surface chemistry and topography of poly(2-hydroxyethyl methacrylate) on the in vitro attachment of human corneal epithelial cells. Journal of Bioactive and Compatible Polymers, 2018, 33, 321-331.	0.8	1
350	Photo-directing chemoepitaxy: the versatility of poly(aryl methacrylate) films in tuning block copolymer wetting. Polymer Chemistry, 2021, 12, 3201-3209.	1.9	1
351	Synthesis, thermal and radiation sensitivities of some linear aromatic polyesters. Polymer International, 1999, 48, 971-979.	1.6	1
352	An ESR Study of the UV Photolysis of Styrene and Maleic Anhydride at 90 K. Journal of Macromolecular Science Part A, Chemistry, 1986, 23, 403-414.	0.4	0
353	Characterization of the Acidic Properties of Mesoporous Aluminosilicates Synthesized from Leached Saponite with Additional Aluminum Incorporation ChemInform, 2003, 34, no.	0.1	Ο
354	Physicochemical and Structural Characterization of Mesoporous Aluminosilicates Synthesized from Leached Saponite with Additional Aluminum Incorporation ChemInform, 2004, 35, no.	0.1	0
355	The Role of Citrate Anions in Prevention of Calcification of Poly(2-hydroxyethyl methacrylate) Hydrogels. ACS Symposium Series, 2007, , 301-316.	0.5	Ο
356	Everything Under the Sun: The 11th Pacific Polymer Conference. Australian Journal of Chemistry, 2010, 63, 1141.	0.5	0
357	Understanding the Diffusion of Dextrans in â€ <sup>~</sup> Click' PNIPAAm Hydrogels. Australian Journal of Chemistry, 2014, 67, 85.	0.5	Ο
358	The chemistry and application of nonchemically amplified (non-CA) chain-scission resists. Frontiers of Nanoscience, 2016, 11, 193-210.	0.3	0
359	Recent Advances in the Determination of Crosslinking and Scission in Irradiated Polymers. , 1991, , 315-325.		0
360	Sustained-release ketamine-loaded lipid-particulate system: in vivo assessment in mice. Drug Delivery and Translational Research, 2021, , 1.	3.0	0